

Attachment performance between micro particles and different sized aerobic granular sludge from outside to inside

Peng, Zhaoxu; Lin, Yuemei; van Loosdrecht, Mark C.M.; de Kreuk, Merle K.

DOI

[10.1016/j.watres.2025.123539](https://doi.org/10.1016/j.watres.2025.123539)

Publication date

2025

Document Version

Final published version

Published in

Water Research

Citation (APA)

Peng, Z., Lin, Y., van Loosdrecht, M. C. M., & de Kreuk, M. K. (2025). Attachment performance between micro particles and different sized aerobic granular sludge: from outside to inside. *Water Research, 280*, Article 123539. <https://doi.org/10.1016/j.watres.2025.123539>

Important note

To cite this publication, please use the final published version (if applicable). Please check the document version above.

Copyright

Other than for strictly personal use, it is not permitted to download, forward or distribute the text or part of it, without the consent of the author(s) and/or copyright holder(s), unless the work is under an open content license such as Creative Commons.

Takedown policy

Please contact us and provide details if you believe this document breaches copyrights. We will remove access to the work immediately and investigate your claim.



Attachment performance between micro particles and different sized aerobic granular sludge - from outside to inside

Zhaoxu Peng^{a,c,*}, Yuemei Lin^b, Mark C.M. van Loosdrecht^b, Merle K. de Kreuk^a

^a Faculty of Civil Engineering and Geosciences, Section Sanitary Engineering, Department of Water Management, Delft University of Technology, Stevinweg 1, Delft, South Holland 2628 CN, the Netherlands

^b Department of Biotechnology, Delft University of Technology, van der Maasweg 9, 2629 HZ, Delft, the Netherlands

^c School of Water Conservancy and Transportation Engineering, Zhengzhou University, Kexue Road 100, Zhengzhou, 450001, China

ARTICLE INFO

Keywords:

Aerobic granular sludge
Particle
Layer
Attach
Amyloid

ABSTRACT

The aerobic granular sludge (AGS) is an emerging technology widely spread, since most organic matters in actual domestic sewage were particulate matters, this study aims to determine whether the attachment between micro particles and different sized AGS was influenced by granule surface area. The attachment of micro particles by different sized AGS (2.0–5.0 mm) were investigated. Furthermore, to simulate the attachment by broken fragments of AGS, complete 4.0–5.0 mm AGS were cut into 2, 4, and 8 pieces, and the attachment performance between the broken pieces and similar sized complete AGS were compared. Fourier transform infrared (FTIR) and fluorescence staining were applied to analyze the chemical bonds and amyloid-glucan like structure of AGS from outside to inside. The results showed the 3.1–4.0 mm AGS had the best surface area attachment of micro particles, followed by the 2.5–3.1 mm AGS. The attachment performance of micro particles was not determined by specific surface area, but was closely related to the surface roughness caused by the amyloid-glucan like structure. The distribution density of amyloid-glucan like structure decreased from outside to inside, and if an granule was broken into pieces during aeration, micro particles were preferential to be attached by the outer layer of the broken pieces from the initial granule. The micro particles attachment showed little relationship with the hydrophilicity of AGS surface, either the outer layer or the inner layer. This study highlighted the crucial role of AGS outer layer in micro particle attachment, particularly the broken pieces from the original AGS outer layer, which facilitate to attach micro particles and contribute to form new granules.

1. Introduction

In the last two decades, aerobic granular sludge (AGS) has emerged as one of the sustainable wastewater treatment technologies (Hamza et al., 2022), which uses the aggregate of microbial origin with excellent settleability (Winkler and Van Loosdrecht, 2022; De Kreuk et al., 2007). Compared to the traditional activated sludge, AGS requires less footprint and energy consumption. Meanwhile, the multiple layered structure (aerobic outer layer, anoxic/anaerobic inner layer) provide the condition to coexist nitrifiers, denitrifiers and phosphate accumulating organisms, which improves the simultaneous removal of COD, nitrogen, and phosphorus (De Kreuk et al., 2005). The AGS are mostly applied in sequential batch reactors under the trade name Nereda® (Pronk et al., 2015). One cycle usually consisted of up-flow simultaneously anaerobic feeding/discharging, aeration, and quick settling (van Dijk et al., 2020).

One of the key strategies to cultivate AGS is to guarantee influent organics is used (or stored) by slowly growing organisms as much as possible during feeding phase (De Kreuk et al., 2010; Winkler et al., 2012).

In the real municipal sewage, most organic matters exist in the form of particles (typically >50 %) (Metcalf and Eddy, 2014; Derlon et al., 2016), and the particle size in black water and grey water concentrated in the 10–150 μm (Hocaoglu et al., 2013). However, the primary treatment in sewage treatment plant had little removal efficiency on the particles smaller than 150 μm (Liu et al., 2016). In order to use particle organics to cultivate AGS, firstly the particle organics must be attached by the AGS, secondly it should be hydrolyzed into smaller products by heterotrophic bacteria. Previous research showed there was a similar distribution of hydrolytic activity in all sized granules (0.5–4.8 mm), and hydrolysis is largely surface-area related (Toja Ortega et al., 2021,

* Corresponding author.

E-mail address: pzx@zsu.edu.cn (Z. Peng).

<https://doi.org/10.1016/j.watres.2025.123539>

Received 25 January 2025; Received in revised form 19 March 2025; Accepted 21 March 2025

Available online 22 March 2025

0043-1354/© 2025 The Author(s). Published by Elsevier Ltd. This is an open access article under the CC BY license (<http://creativecommons.org/licenses/by/4.0/>).

2022). Indicating the smaller granules with larger specific surface area had better hydrolytic activity. Meanwhile, the extracellular polymeric substances (EPS) play a crucial role in maintaining the structural integrity, rheological properties, functional stability of AGS, and can influence the physicochemical characteristics of the biomass, such as AGS size, stability, adsorption capacity. Actually, the extracted EPS products from AGS can be used as biosorbent materials (Feng et al., 2021, 2024). However, the research on the attachment between micro particles and different sized AGS is still limited, as well as the effect of EPS components.

Actually, after quick settling the larger granules are more prone to end up in the bottom of sludge bed, which has priority to uptake influent organics than smaller granules (van Dijk et al., 2022). During the plug flow feeding many sewage micro particles are accumulated nearby the bottom (Layer et al., 2020a), and the accumulated micro particles will be mixed into the bulk during aeration. Then there will be a competition to attach the suspended micro particles between different sized granules. Sometimes pieces were break away from granules by collision or liquid shear (Gjaltema et al., 1995), and the separated pieces will also compete to attach the suspended particles. Whether the attachment performance is also largely surface-area related like hydrolytic activity? Or the little pieces had better attachment ability? Some research found the particles attach preferentially to the flocs during aeration (Layer et al., 2020b), while some sludge flocs (<0.20 mm) in AGS systems were pin-point flocs (Morgenroth et al., 1997), which were different from traditional activated sludge flocs.

The main objective of this study was to better understand the attachment between influent micro particles and AGS. First we explored whether the attachment performance of micro particles by different sized AGS were surface-area related; Second, we cut large AGS into little pieces, and compared the attachment performance between the broken pieces and similar sized complete AGS; Furthermore, we investigated the chemical bonds and amyloid-glucan like structure of granules from outside to inside. Based on these observation, the attachment process between micro particles and granules was further evaluated, it is hoped to provide a detailed understanding of the transition of influent particles

in Nereda®.

2. Materials and methods

2.1. Sludge sampling and processing

The aerobic granules were collected from a Nereda® sewage treatment plant (Utrecht, The Netherlands) with the designed flow and sludge loading rate of $74,700 \text{ m}^3 \cdot \text{d}^{-1}$ and $0.05 \text{ kgCOD} \cdot \text{kgVSS}^{-1} \cdot \text{d}^{-1}$. The distribution of the mixed liquor suspended solids (MLSS) with biomass size was $11.42 \pm 0.03 \%$ (<0.2 mm), $17.71 \pm 0.24 \%$ (0.2–1.0 mm), $32.03 \pm 0.10 \%$ (1.0–2.0 mm), $22.77 \pm 0.07 \%$ (2.0–3.1 mm) and $16.07 \pm 0.05 \%$ (>3.1 mm). The sludge was gently washed by tap water several times until the supernatant was clean. Then the sludge mixture was sequentially filtered by stainless steel sieves with the pore size of 5.0 mm, 4.0 mm, 3.1 mm, 2.5 mm, 2.0 mm, respectively. The fractions of 2.0–2.5 mm, 2.5–3.1 mm, 3.1–4.0 mm, and 4.0–5.0 mm were collected in two ways (Fig. 1). The first way is picking up a specific number of granules from each fraction for test A, B, C, D, E, F and G (red hand), during which the attachment was quantified through counting the particles attached on the biomass; the second way is picking up 40 mL filtrate solid from each fraction for test a, b, c, d, e, f and g (green hand), during which the attachment was quantified through counting the particles left in the bulk.

2.2. Micro particles solution and AGS cutting

The 250 μm fluorescent microbeads (Cospheric, WTW d-82,362) with the density of $1.02 \text{ g} \cdot \text{mL}^{-1}$ were used to simulate the non-biodegradable particles. Two solutions were prepared as follows: Solution I was for Test A B C D E F G. Five drops of red latex microbeads were ground by a mortar, then it was added into 1 L mili-Q Water to make a solution of $5967 \pm 874 \text{ particles} \cdot \text{L}^{-1}$ with the size of $86 \pm 49 \mu\text{m}$. Solution II was for Test a b c d e f g. One drop of green latex microbeads was ground by a mortar to prepare a solution of $1300 \pm 283 \text{ particles} \cdot \text{L}^{-1}$ with the size of $95 \pm 46 \mu\text{m}$.

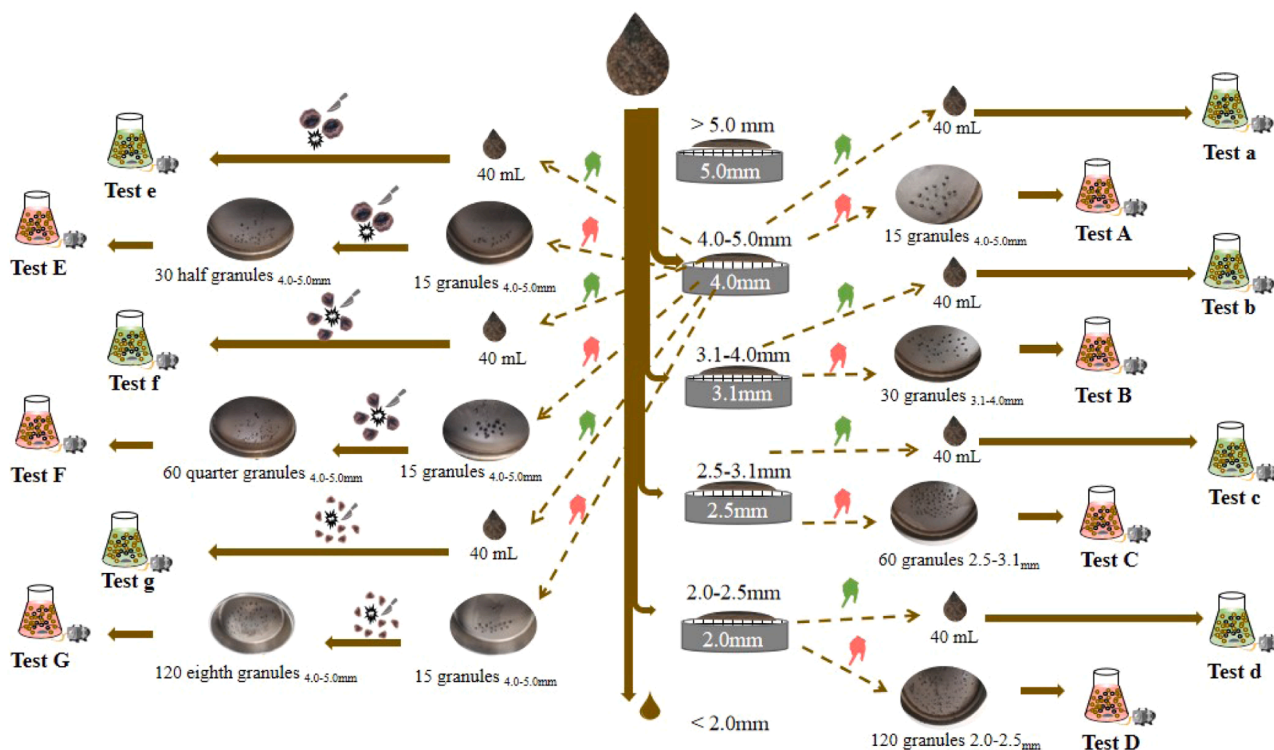


Fig. 1. Experiment set up.

AGS cutting process: First, the 4.0–5.0 mm AGS were washed by tap water, and placed on a stainless steel sieve (pore size=200 μm); Second, each AGS was carefully cut into 2 pieces (test e and E), 4 pieces (test f and F), and 8 pieces (test g and G) with an art knife, respectively. To minimize human error, if one AGS cutting was failed, another AGS would be cut instead.

2.3. Attachment tests

The experiment consisted of 2 parts (each part had 7 batch tests), solution I and solution II were used in the uppercase part and lowercase part, respectively (Table 1). During each batch test 200 mL solution was dropped into a 250 mL conical flask, followed by the addition of biomass. Then the mixture was aerated for 60 min (2.0 L \cdot min $^{-1}$). The biomass in the uppercase part and lowercase part were a specific number of AGS (granular pieces) and 40 mL filtrate, respectively. In the uppercase part, the tests A, B, C, D compared the micro particles attachment by different sized AGS, and tests B/E, C/F, D/G compared the micro particles attachment by complete AGS and similar sized granular pieces. The procedure of lowercase part was the same.

2.4. Micro particles count

Batch test with solution I: After each batch test, 15 granules (or pieces) were picked up randomly to count the attached micro particles, and they were divided into 3 groups randomly. For each group, the digital microscope (VHX-5000) was used to observe the granules (pieces) and take pictures for every attached micro particle. The area, perimeter of each particle was measured by Image J. The equivalent diameter is calculated based on the circle with the same area of the particle.

Batch test with solution II: Samples were collected at 10 min, 30 min and 60 min during aeration. The sieves with pore sizes of 3.1 mm, 2.0 mm, 1.0 mm and 200 μm were stacked from top to the bottom, followed by pouring 10 mL sample for sequential filtration. Then the filtered solids were rinsed by tap water while continuously shaking the sieves. At last all the mixture passed through the 200 μm sieve was observed by digital microscope (VHX-5000). Any observed micro particles was photographed, then all the images were analyzed by a deep learning method to quantify the number, shape and area of the observed micro particles (Jia et al., 2024).

2.5. Analytical methods

2.5.1. FTIR

The outer aerobic layer, inner anaerobic layer, and cross section of granules (pieces) before batch test were analyzed by Fourier transform infrared (FTIR). The biomass for FTIR analysis was frozen under $-80\text{ }^{\circ}\text{C}$ (DW-60L80) for 2 h before lyophilized by a freeze drier (YTLG-10A) for

24 h. FTIR spectra was carried out by a FTIR spectrometer (Model FTIR-650) to identify any functional groups on the surface. For each sized biomass, two samples were analyzed at least.

2.5.2. Fluorescence staining

Fluorescence recording of Ebba680 bound structure (amyloid-glucan like) in granular sludge was done as follows: (1) Fix the biomass with ice-ethanol at room temperature for 5 min; (2) Take out the biomass, and equilibrate it in phosphate buffer saline (PBS) for 5 min; (3) Dilute BbbaBiolight 680 in PBS with 1:1000; (4) Take out the biomass again, and incubate it in the diluted BbbaBiolight solution under room temperature for 30 min; (5) Mount the biomass and seal the coverslip onto the slide. The sample was observed by Olympus fluorescence microscope (BX63) with Cy3 filter set. The excitation and emission wavelengths were 530 nm and 680 nm, respectively.

2.5.3. EPS

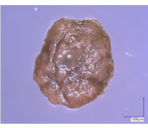
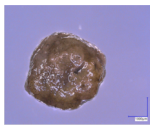
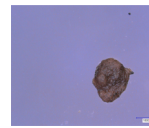
A sample of 3 g wet granule_{4.0–5.0 mm} were collected, and the outer aerobic part (light-colour) and inner anaerobic part (dark-colour) were carefully separated by an art knife one by one. The separated outer and inner parts, as well as the complete granule_{4.0–5.0 mm} were used to extract the stratified extracellular polymeric substances (EPS) (loosely bound-EPS (LB-EPS) and tightly bound-EPS (TB-EPS)) by centrifugation and mild-harsh heat method (Guo et al., 2020). The protein (PN) concentration and polysaccharide (PS) concentration were determined by a modified Lowry method with bovine serum albumin (Sigma, USA) as standard (Frolund et al., 1995) and phenol-sulfuric acid assay with glucose (Sigma, USA) as standard (Dubois et al., 1956), respectively.

3. Results

3.1. Attach performance

The attachment performance of micro particles by different sized granules were compared (Fig. 2). In this study, specific attachment was used to represent the attachment performance, which was determined by the number of attached micro particles by per unit mass of biomass. The density of AGS are 1.026–1.028 g \cdot cm $^{-3}$ (Van den Berg et al., 2022), to calculate the specific attachment the density of all sized granules were assumed as 1.027 g \cdot cm $^{-3}$. The specific surface area increased with the decrease of granule size, but the average attachment performance during aeration showed limited relationship with the specific surface area. The granules_{3.1–4.0 mm} exhibited the best average attachment performance in both experimental parts. In addition, the attachment was selective to capture smaller micro particles. The average particle size of solution I was $86\pm 49\text{ }\mu\text{m}$, while the average attached particles were only $38\pm 22\text{ }\mu\text{m}$, and the granules with better attachment performance tended to capture larger particles (Fig. 2(a)). Furthermore, particle shape could also influence the attached particle size. The average circularity of the

Table 1
Operation of batch test.

No Morphology	A / a	B / b	C / c	D / d	E / e	F / f	G / g
							
Sieve pore (mm)	4.00–5.00	3.10–4.00	2.50–3.10	2.00–2.50	4.00–5.00	4.00–5.00	4.00–5.00
Granule (piece) number/ Filtrate volume (mL)	15/ 40	30/ 40	60/ 40	120/ 40	30/ 40	60/ 40	120/ 40

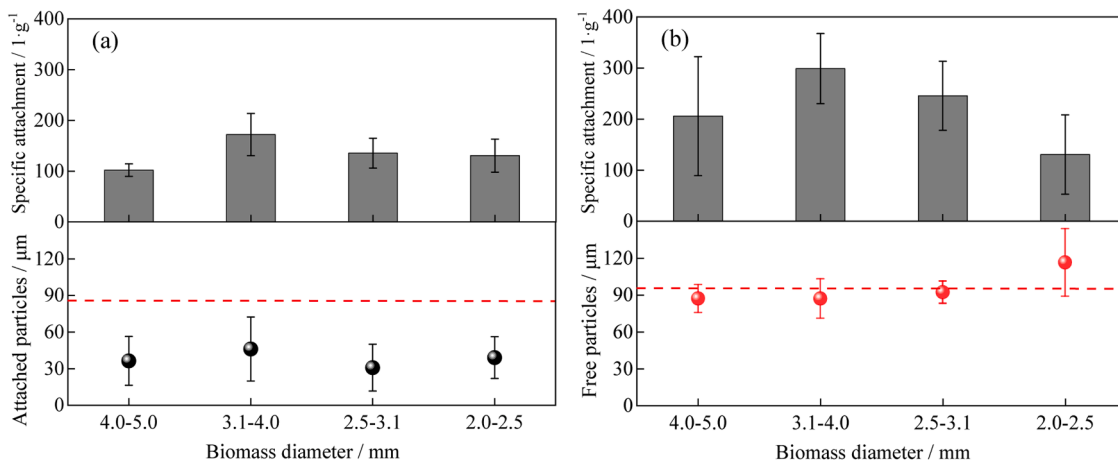


Fig. 2. The attachment performance of micro particles by different sized granules (a) Solution I; (b) Solution II.

micro particles in solution I was 0.73 ± 0.11 , and the attached particle size increased with the decrease of circularity, indicating the slender particles were more prone to be attached. The average particle size of solution II was $95 \pm 46 \mu\text{m}$, the granules with worse attachment performance tended to capture smaller particles, resulting more larger particles left in the bulk (Fig. 2(b)). The difference of specific attachment between Fig. 2(a) and Fig. 2(b) was from the MLSS. In the tests with solution I only a few granules were in the bulk, so it was difficult to attach micro particles. While in the tests with solution II the MLSS was $2000\text{--}3000 \text{ mg}\cdot\text{L}^{-1}$, so the micro particles could be attached more sufficiently.

The micro particles attachment performance between complete granules and similar sized pieces were shown in Fig. 3. The specific surface area of pieces_{3.57 mm} (a half of granules_{4.00–5.00 mm}) and pieces_{2.83 mm} (a fourth of granules_{4.00–5.00 mm}) were 1.67 and $2.33 \text{ mm}^2\cdot\text{mm}^{-3}$, which were similar to those of granules_{3.1–4.0 mm} and granules_{2.5–3.1 mm}, while both the granules_{3.1–4.0 mm} and granules_{2.5–3.1 mm} exhibited better attachment performance, either in solution I or solution II. The specific attachment of granules_{3.1–4.0 mm} (granules_{2.5–3.1 mm}) were 89.73% (7.21%) and 63.16% (1.84%) bigger than those of pieces_{3.57 mm} (pieces_{2.83 mm}) in solution I and solution II, respectively. It seems compared to the external surface, the internal surface (cross-section) exhibited lower attachment capacity for micro particles. However, the granules_{2.0–2.5 mm} exhibited worse attachment performance than pieces_{2.25 mm} (an eighth of granules_{4.00–5.00 mm}) in both solutions. Actually, to divide one granule_{4.0–5.0 mm} into 8 pieces_{2.25 mm} required 3 cuts, and each cut would affect the structural stability. Therefore,

sometimes the inner anaerobic core or some surface fragments will be separated from the granules during aeration, and the available attached area (especially the outer layer surface) increased. This increase was more obvious in the batch test with solution II (Fig. 3(b)), because the inner anaerobic core was stronger than the outer aerobic layer, and more outer layer fragments would be peeled off under higher MLSS condition (Tijhuis et al., 1994).

3.2. FTIR of the outer surface and cross section of granules

The FTIR spectra of the outer surface of each sized granules were shown in Fig. 4(a). For the granules_{2.5–3.0 mm}, the typical adsorption peak frequencies were from lipid ($2930, 3290, \text{cm}^{-1}$), protein ($1653, 1560, \text{cm}^{-1}$), polysaccharidess ($1048, \text{cm}^{-1}$) (Zhou et al., 2023). For the granules_{3.1–4.0 mm}, the typical adsorption peak frequencies were from protein ($1555, \text{cm}^{-1}$), polysaccharidess ($1054, 1071, \text{cm}^{-1}$). For the granules_{4.0–5.0 mm}, the typical adsorption peak frequencies were from protein ($1545, 1653, \text{cm}^{-1}$), polysaccharidess ($1045, \text{cm}^{-1}$) (Liu et al., 2015). The FTIR spectra scanned at different places of the outer surface of granules_{3.1–4.0 mm} were similar, while for the granules_{2.5–3.1 mm} and granules_{4.0–5.0 mm} the FTIR spectra at different places are different. This indicated that the surface of granules_{3.1–4.0 mm} was relatively homogeneous, while the others were heterogeneous. The porosity inside AGS also showed similar phenomenon, which became more heterogeneous from outside to inside because the fragments close to the core was denser (Zaghloul and Achari, 2022). Therefore, it's possible that during the growth process of granules (such as from granules_{2.5–3.1 mm} to

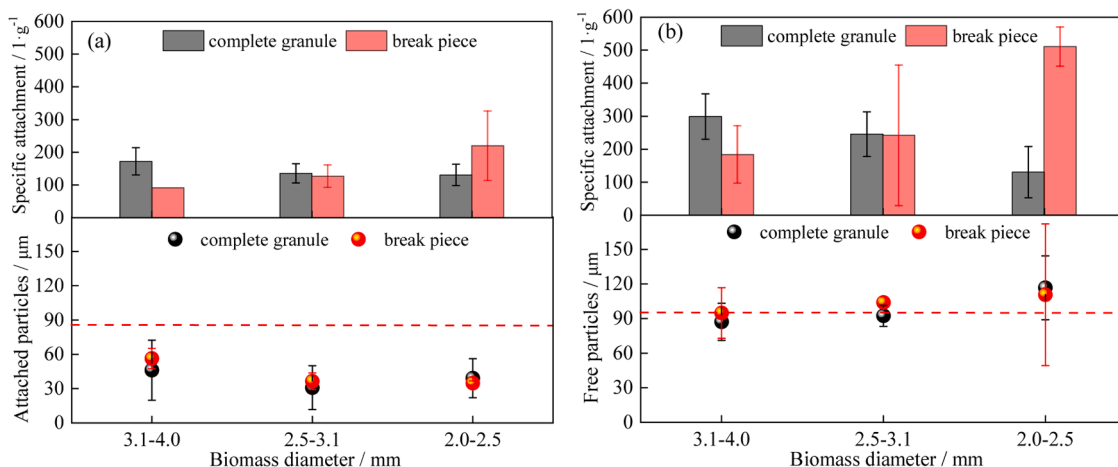


Fig. 3. The attachment of complete granules and pieces under similar size (a) Solution I; (b) Solution II.

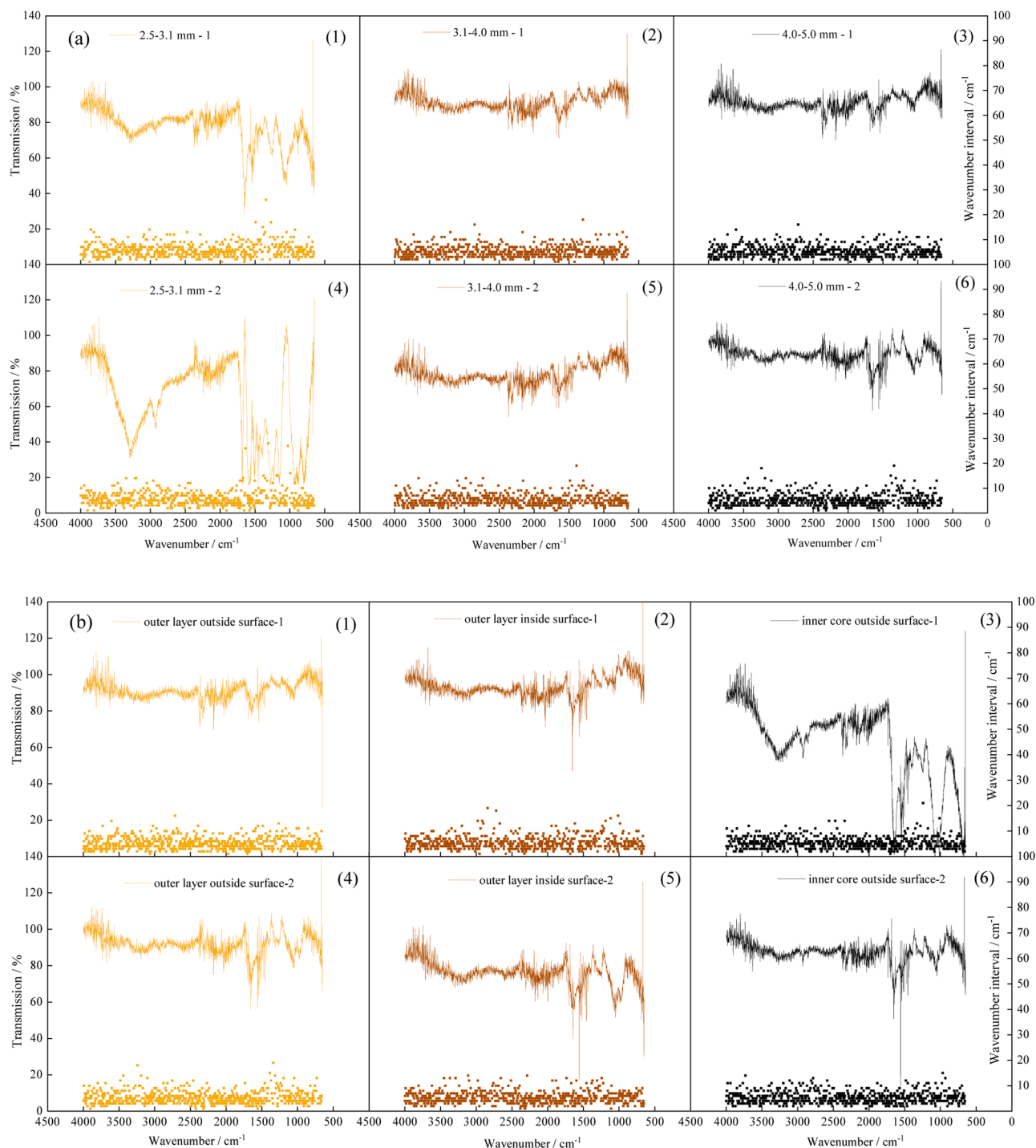


Fig. 4. FTIR of outer surface and cross section of granules (a) outer surface of different sized granules; (b) from outer surface to inner surface (granules_{4.0–5.0 mm}).

granules_{3.1–4.0 mm}), the newly growing biomass on the outer surface is more loosely, leading to a relatively homogeneous surface. However, when the granules become too big (such as granules_{4.0–5.0 mm}), different parts of its surface suffered greater differences in impact during aeration, resulting in a tendency towards heterogeneous.

The granules_{4.0–5.0 mm} was used to investigate the morphology from outside to inside. The FTIR spectra of the outer layer outside surface, outer layer inside surface and inner core outside surface were shown in Fig. 4(b). For the outer layer outside surface, the typical adsorption peak frequencies were from protein (1545, 1653, cm^{-1}), polysaccharides (1045, cm^{-1}) (Yang et al., 2023). For the outer layer inside surface, the typical adsorption peak frequencies were from proteins (1653, 1559

cm^{-1}), polysaccharides (1050 cm^{-1}). For the inner core outside surface, the typical adsorption peak frequencies were from proteins (1648, 1653, cm^{-1}), polysaccharides (1012, 1050, 1078, cm^{-1}) (Li et al., 2015). There was always obvious boundary between the outer layer (light brown) and inner core (deep black). The reason might be the outer regions were predominantly loose aerobic or facultative aerobic zones, while the interior constituted dense anaerobic zones. It was interesting to observe some outer layer outside surface (Fig. 4(b)(1)) was similar to the outer layer inside surface (Fig. 4(b)(2)), indicating the structure on the two surfaces of aerobic (facultative aerobic) zones were the same. While some outer layer inside surface (Fig. 4(b)(5)) was similar to the inner core outside surface (Fig. 4(b)(6)), since they were tightly

interconnected.

In this study no smooth was conducted for the FTIR spectra, and numerous little peaks were observed. These little peaks may result from the concave-convex structure on the surface of granules, and the wavenumber interval of these little peaks is inversely proportional to the distribution density of the concave-convex structure. The distribution of

wavenumber interval were shown in Fig. 4. The average wavenumber interval of granules_{4.0-5.0 mm}, granules_{3.1-4.0 mm}, and granules_{2.5-3.1 mm} were $5.21 \pm 2.36 \text{ cm}^{-1}$, $5.19 \pm 2.26 \text{ cm}^{-1}$ and $5.58 \pm 2.82 \text{ cm}^{-1}$, respectively, indicating the surface of granules_{3.1-4.0 mm} exhibited the densest distribution of concave-convex structure. This was consistently with its best attachment performance. For the granules_{4.0-5.0 mm}, the average

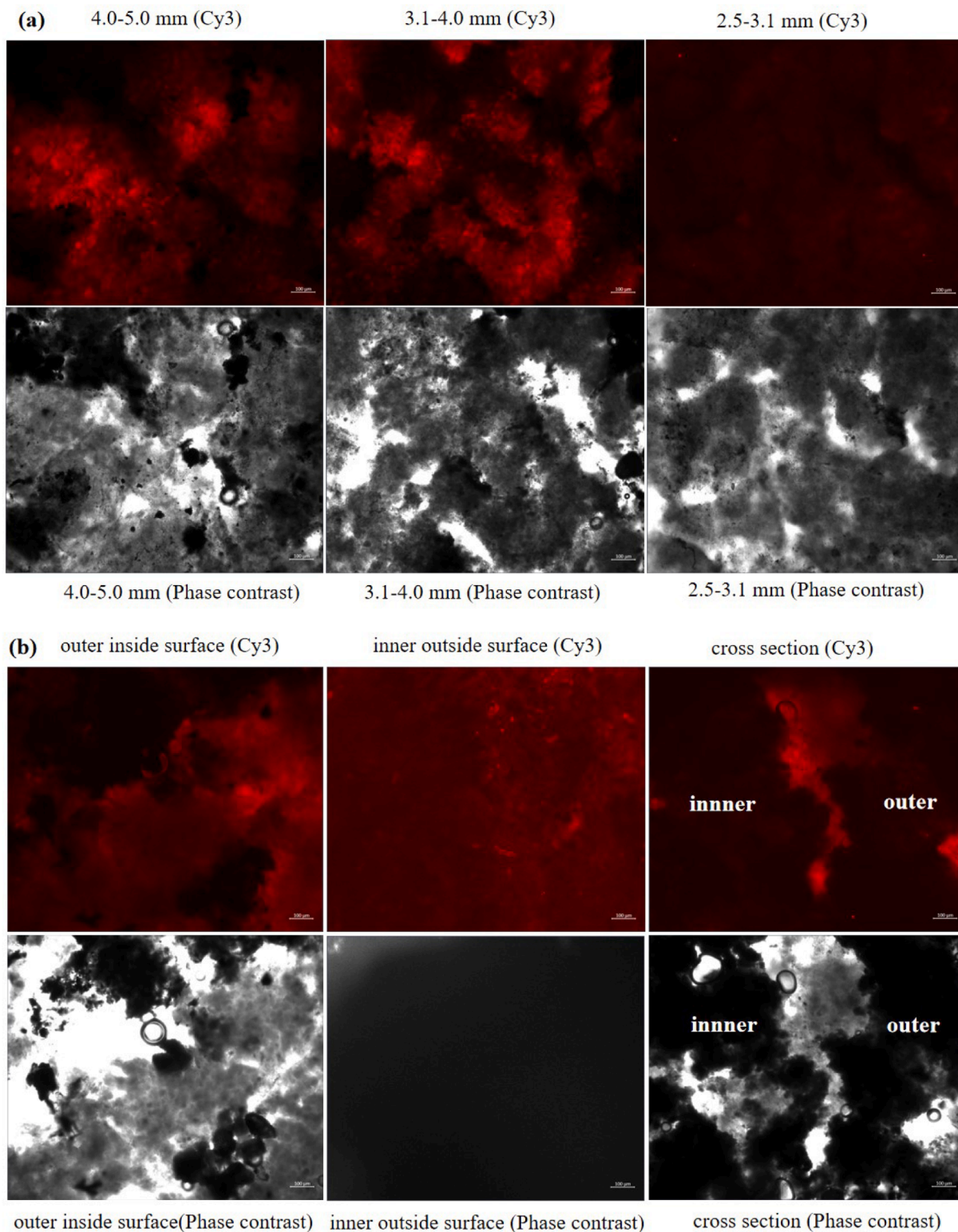


Fig. 5. amyloid-glucan like structure distribution on the surface of granules (a) the surface of different sized granules; (b) the surface of granules_{4.0-5.0 mm} from outside to inside.

wavenumber interval between each little peak increased from outer layer outside surface ($5.21 \pm 2.36 \text{ cm}^{-1}$) to outer layer inside surface ($5.35 \pm 2.39 \text{ cm}^{-1}$), and further to inner core outside surface ($5.36 \pm 2.26 \text{ cm}^{-1}$). This indicated the concave-convex structure on the surface of inner anaerobic zones was less density distributed, so the particles attachment capacity of cross-section was less than outer layer surface, which explained the attachment performance between complete granules and similar sized pieces.

3.3. Amyloid-glucan like structure on the surface of granules

The Cy3 filter and Phase contrast pictures of different sized granules were shown in Fig. 5(a), the amyloid-glucan like structure on the surface of granules showed fluorescent highlight red spots. For the granules $_{4.0-5.0 \text{ mm}}$ most gray and white area in Phase contrast pictures were stained red in Cy3 picture, while only a part of gray area displayed highlight red spots. For the granules $_{3.1-4.0 \text{ mm}}$ the proportion of highlight red area was bigger, and almost all gray area in Phase contrast pictures displayed highlight red spots in Cy3 picture. For the granules $_{2.5-3.1 \text{ mm}}$, almost none highlight red spots were observed. It seemed the surface roughness caused by the amyloid-glucan like structure might determine the attachment performance of micro particles. The more amyloid-glucan like structure distributed, the better the attachment performance was. This indicated the amyloid-glucan like structure presented by fluorescence staining was similar to the structure reflected by the wavenumber interval between each little peak in FTIR spectra.

The Cy3 filter and Phase contrast pictures of granules $_{4.0-5.0 \text{ mm}}$ from outside to inside were shown in Fig. 5(b). Compared with the outer outside surface (Fig. 5(a)), little highlight red spots were observed on the outer inside surface, indicating the amyloid-glucan like structure occupation decreased from outside to the inside. For the inner outside surface, although most black area in Phase contrast pictures were stained light red in Cy3 picture, only a few highlight red spots were observed. For the cross section, it was obvious to see there was almost none highlight red spots in the inner, and some in the outer just as the outer inside surface. These observation verified that the roughness produced by the amyloid-glucan like structure improved the attachment performance of micro particles.

4. Discussion

4.1. The optimal granule diameter for micro particles attachment

Although the hydrolytic activity of AGS is largely surface-area related (Toja Ortega et al., 2022), the micro particles attachment is determined by not only the available surface-area, but also the surface characteristics. Since most organics in actual wastewater exist as micro particles (Derlon et al., 2016), to cultivate AGS the influent micro particle organics must be attached by the biomass firstly, then consequently be hydrolyzed to soluble organics. In Nereda® the larger granules settled to the bottom were priority to attach the influent particle organics during bottom feeding phase (Toja Ortega et al., 2021). However, in continuous flow systems the solution was completely mixed, and the smaller biomass are more prone to attach influent particle organics due to the bigger specific surface area (Haaksman et al., 2023; Wei et al., 2020). That is one of the reasons why it is difficult to cultivate larger granules in continuous flow systems. Although the biomass mixture collected from full-scale Nereda® plant also contained some fraction smaller than 0.2 mm, the major constituents of biomass concentrated in 1–3 mm due to the unique operational and biomass selection methods (Quoc et al., 2021). Actually, once small granules were formed in Nereda®, they easily grow into larger granules. According to this study, the granules $_{3.1-4.0 \text{ mm}}$ had the best attachment performance with the micro particles. When the AGS was <3.1–4.0 mm, its attachment capacity of micro particles improved with an increase in AGS size.

4.2. The effect of broken AGS fragments on the attachment performance

Granules collide with each other during aeration randomly, and some fragile or unstable parts will break into little pieces. How will these small pieces affect the formation of AGS? The half granule $_{4.0-5.0 \text{ mm}}$, quarter granule $_{4.0-5.0 \text{ mm}}$ and eighth granule $_{4.0-5.0 \text{ mm}}$ with attached micro particles after aeration were shown in Fig. 6. Some particles were attached by the outer layer (Fig. 6(a),(c)), and some were by the inner core (Fig. 6(b)). Since the structural stability was affected by the cutting procedure, some fragile parts were separated from the granules during aeration. The granule depicted in Fig. 6(d) showed the surface with numerous abrasions. Sometimes the inner black core (Fig. 6(d)) was completely separated from the outer layer (Fig. 6(e)), this would increase the available area for attachment. And sometimes a huge gap was left on the outer layer (Fig. 6(f)), the hollow gap also provided an ideal site to attach micro particles (Tijhuis et al., 1994). When treating the real sewage, if the attached particles were non-biodegradable, they were easily to be enveloped by the newly growing biomass around (Pronk et al., 2015).

For the half granule $_{4.0-5.0 \text{ mm}}$ and quarter granule $_{4.0-5.0 \text{ mm}}$, the area ratio of outer layer to inner core (O/I) were 2.29 and 1.19, and the number ratio of the attached particles by outer layer to inner core were 2.67 and 1.56 in the batch tests with solution I, which verified again the outer layer were more prone to attach micro particles. Furthermore, although the O/I of eighth granule $_{4.0-5.0 \text{ mm}}$ was only 0.83, while the number ratio of the attached particles by outer layer to inner core was as high as 3.00. The abnormally high increase was due to many particles were attached onto the newly generated surface at the outer layer's abrasions. This implied if a granule was broken into fragments during aeration, the fragmented pieces not only can serve as nuclei to attach micro particles to form new AGS (Van Dijk et al., 2022), but also has the potential to generate more fragments for micro particle attachment, especially from its detached outer layer. Furthermore, the EPS contents of the outer layer and inner core were measured. The PN and PS of the LB-EPS in the outer layer, inner core and whole granules were 3.52 and 0.46 $\text{mg}\cdot\text{g}^{-1}$, 34.45 and 0.72 $\text{mg}\cdot\text{g}^{-1}$, 29.85 and 0.59 $\text{mg}\cdot\text{g}^{-1}$, respectively. And in the TB-EPS they were 21.14 and 6.47 $\text{mg}\cdot\text{g}^{-1}$, 34.46 and 3.70 $\text{mg}\cdot\text{g}^{-1}$, 26.86 and 4.25 $\text{mg}\cdot\text{g}^{-1}$, respectively. The PN and PS of the whole granules were always between the outer layer and inner core. Specifically, the PN to PS ratio (PN/PS) of LB-EPS were bigger than those of TB-EPS, no matter which part, and the PN/PS of inner core were significantly bigger than those of outer layer in both LB-EPS and TB-EPS. This implied the inner parts of AGS was more hydrophobic (Feng et al., 2021). Since the micro particles used in this study were hydrophobic, and the surface of outer layer of AGS were usually hydrophilic (Lin et al., 2017), there was limit relationship between the micro particles attachment and the hydrophilicity of AGS surface.

The organic micro pollutants could be adsorbed onto the AGS by the interactions between ionized molecules/charged sludge surface and the affinity to the organic phase (Burzio et al., 2024), both the properties of organics and AGS could determine the attachment performance. Actually, the granules derived EPS have proven to be a good biosorbent through the physicochemical interactions between functional groups and adsorbates. In actual wastewater, the metal ions such as Cd^{2+} , Pb^{2+} could be removed by the complexation of -COOH and -OH (Li et al., 2017). Feng et al. (2024) found the electrostatic interaction was important for the organic micro pollutants adsorption in AGS systems, and there was significant adsorption for 6 positively and 4 zwitterionic charged pharmaceuticals by AGS. Larger AGS exhibited better attachment performance probably due to the increased EPS. However, in our study the surface charge of the fluorescent microbeads was negative, but its attachment by AGS were also good. It was found the roughness caused by amyloid-glucan like structure determined the attachment performance, and this structure was normal distributed on the surface of AGS (Lin et al., 2017).

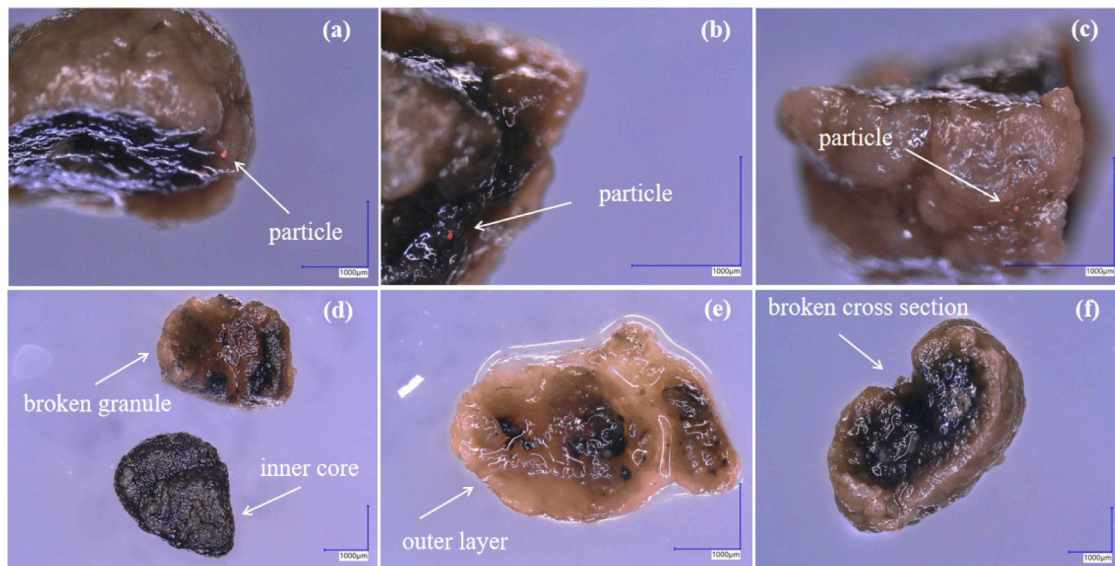


Fig. 6. Biomass fragments after aeration (a) half granule_{4.0-5.0 mm}; (b) quarter granule_{4.0-5.0 mm}; (c) eighth granule_{4.0-5.0 mm}; (d) incomplete granule and separated inner core; (e) separated outer layer; (f) broken cross section.

4.3. The competition to attach micro particles between different sized granules

During the up-flow feeding phase, although the bottom larger granules had the priority to attach influent particles, the upper smaller granules still had the opportunity to attach particles when the up-flow velocity was close to $5 \text{ m}\cdot\text{h}^{-1}$ (Prong et al., 2015). So to prevent most particle organics accumulating around the bottom, it is reasonable to increase up-flow velocity under acceptable value (such as $2\text{--}3 \text{ m}\cdot\text{h}^{-1}$). During aeration phase, the competition to attach micro particles between different sized granules was mainly determined by the distribution of different sized biomass in MLSS. In addition, the other sized AGS were also cut into two parts to observe the cross section (Fig. 7). When the granule diameter was $1.00\text{--}5.00 \text{ mm}$, the thickness of outer layer showed a little positive relationship with the diameter (0.719). For the granules_{1.00-2.00 mm} the thickness of aerobic layer were $0.20\text{--}0.35 \text{ mm}$. It was interesting to observe almost all outer aerobic layer was thicker than 0.20 mm , which was determined by the penetration depth of DO (Layer et al., 2020b). So if a granule was too small such as lower than

0.50 mm , it was difficult to form anaerobic/anoxic environment inside. The granule diameter showed negative relationship with both the ratios of outer layer to inner core thickness (-0.670) and outer layer to inner core volume (-0.615), indicating more anaerobic fraction was formed inside larger granules.

When a Nereda® plant started to cultivate granules, it is considerable to selectively discharge flocs to guarantee more influent particle organics attached by larger biomass. The dominant granules should be larger than 0.50 mm to ensure simultaneous nitrogen and phosphorus removal. Once the granules grown up to 2.0 mm , they will increase to 4.0 mm easily. However, the metabolism rate inside large granules was inhibited by mass transfer (Van de Berg et al., 2020), and they always exhibit lower activity and energy-consuming mixing (Long et al., 2019), so sometimes large granules should be deliberately discharged in practical AGS engineering.

This study focused on the short-term attachment behavior of non-biodegradable micro particles by different sized AGS. However, the accumulation of non-biodegradable micro particles such as micro plastics would inhibit the nitrogen removal performance in biological

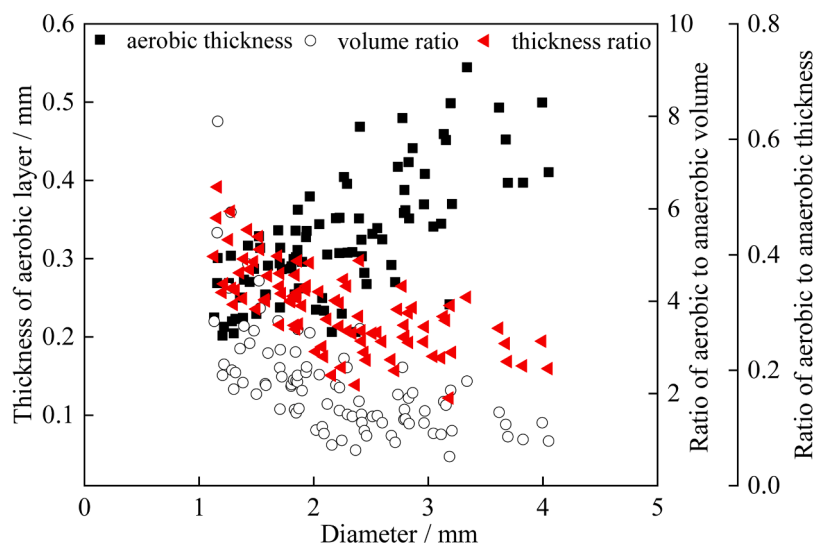


Fig. 7. Effect of granule diameter on the thickness of aerobic layer.

wastewater treatment systems (Zhang et al., 2025). Furthermore, the impact of micro particles attachment on enzyme variations corresponding to microbial change during long-term still required investigation in the future.

5. Conclusions

The attachment of micro particles by AGS was not surface-area related. The roughness caused by amyloid-glucan like structure on the surface exhibited close relationship with the attachment performance. The granules_{3.1–4.0 mm} showed the best attachment performance with its surface occupied by the largest proportion of an amyloid-glucan like structure, as well as its surface was the most homogeneous. From the outside to the inside of granules, fewer amyloid-glucan like structure were observed. When some fragile parts separated from granules during aeration, most micro particles were preferential to be attached by the outer layer, especially the newly formed outer layer's abrasions. Whether these attached non-biodegradable particles can stay outside all the time, or will they gradually “move” inside with the AGS growth are need to be investigated further.

CRedit authorship contribution statement

Zhaoxu Peng: Writing – review & editing, Writing – original draft, Validation, Methodology, Investigation, Data curation, Conceptualization. **Yuemei Lin:** Writing – original draft, Validation, Resources, Methodology, Investigation, Data curation, Conceptualization. **Mark C. M. van Loosdrecht:** Validation, Conceptualization. **Merle K. de Kreuk:** Validation, Supervision, Resources, Methodology, Data curation, Conceptualization.

Declaration of competing interest

The authors declare that they have no known competing financial interests or personal relationships that could have appeared to influence the work reported in this paper.

Acknowledgments

This research was supported by the China Scholarship Council (No. 202107045010). We thank to the colleagues of water lab for their great help, especially to Armand Middeldorp for the use of every equipment. We also thank Mark Stevens for his help during sampling and discussion in the Utrecht sewage treatment plant.

Data availability

Data will be made available on request.

References

- Burzio, C., Mohammadi, A.S., Smith, S., Abadikhah, M., Svahn, O., Modin, O., Persson, F., Wilen, B.M., 2024. Sorption of pharmaceuticals to foam and aerobic granular sludge with different morphologies. *Resour. Environ. Sustain.* 15, 100149.
- De Kreuk, M.K., Heijnen, J.J., Van Loosdrecht, M.C.M., 2005. Simultaneous COD, nitrogen, and phosphate removal by aerobic granular sludge. *Biotechnol. Bioeng.* 90 (6), 761–769.
- De Kreuk, M.K., Kishida, N., Tsuneda, S., Van Loosdrecht, M.C.M., 2010. Behavior of polymeric substrates in an aerobic granular sludge system. *Water Res.* 44 (20), 5929–5938.
- De Kreuk, M.K., Kishida, N., Van Loosdrecht, M.C.M., 2007. Aerobic granular sludge—state of the art. *Water Sci. Technol.* 55 (8–9), 75–81.
- Derlon, N., Wagner, J., da Costa, R.H.R., Morgenroth, E., 2016. Formation of aerobic granules for the treatment of real and low-strength municipal wastewater using a sequencing batch reactor operated at constant volume. *Water Res.* 105, 341–350.
- Dubois, M., Gilles, K.A., Hamilton, J.K., Rebers, P.T., Smith, F., 1956. Colorimetric method for determination of sugars and related substances. *Anal. Chem.* 28 (3), 350–356.
- Frolund, B., Griebe, T., Nielsen, P.H., 1995. Enzymatic-activity in the activated-sludge floc matrix. *Appl. Microbiol. Biotechnol.* 43 (4), 755e761.
- Feng, C., Lotti, T., Canziani, R., Lin, Y., Tagliabue, C., Malpei, F., 2021. Extracellular biopolymers recovered as raw biomaterials from waste granular sludge and potential applications: a critical review. *Sci. Total Environ.* 753, 142051.
- Feng, Z.L., Schmitt, H., Van Loosdrecht, M.C.M., Sutton, N.B., 2024. Sludge size affects sorption of organic micropollutants in full-scale aerobic granular sludge systems. *Water Res.* 267, 122513.
- Gjaltema, A., Tjihuis, L., Van Loosdrecht, M.C.M., 1995. Detachment of biomass from suspended nongrowing spherical biofilms in airlift reactors. *Biotechnol. Bioeng.* 46, 258–269.
- Guo, H., Felz, S., Lin, Y., van Lier, J., De Kreuk, M.K., 2020. Structural extracellular polymeric substances determine the difference in digestibility between waste activated sludge and aerobic granules. *Water Res.* 101, 115924.
- Haaksman, V.A., Schouteren, M., Van Loosdrecht, M.C.M., Pronk, M., 2023. Impact of the anaerobic feeding mode on substrate distribution in aerobic granular sludge. *Water Res.* 233, 119803.
- Hamza, R., Rabii, A., Ezzahraoui, F.-z., Morgan, G., Iorhemen, O.T., 2022. A review of the state of development of aerobic granular sludge technology over the last 20 years: full-scale applications and resource recovery. *Case Stud. Chem. Environ. Eng.* 5.
- Hocaoglu, S.M., Orhon, D., 2013. Particle size distribution analysis of chemical oxygen demand fractions with different biodegradation characteristics in black water and gray water. *CLEAN - Soil, Air, Water* 41 (11), 1044–1051.
- Jia, T., Peng, Z., Yu, J., Piaggio, A., Zhang, S., De Kreuk, M.K., 2024. Detection the interaction between microparticles and biomass in biological wastewater treatment process with Deep learning method. *Sci. Total Environ.* 951, 175813.
- Layer, M., Bock, K., Ranzinger, F., Horn, H., Morgenroth, E., Derlon, N., 2020a. Particulate substrate retention in plug-flow and fully-mixed conditions during operation of aerobic granular sludge systems. *Water Res* X 9, 100075.
- Layer, M., Villodres, M.G., Hernandez, A., Reynaert, E., Morgenroth, E., Derlon, N., 2020b. Limited simultaneous nitrification-denitrification (SND) in aerobic granular sludge systems treating municipal wastewater: mechanisms and practical implications. *Water Res* X 7, 100048.
- Li, N., Wei, D., Wang, S., Hu, L., Xu, W., Du, B., Wei, Q., 2017. Comparative study of the role of extracellular polymeric substances in biosorption of Ni (II) onto aerobic/anaerobic granular sludge. *J. Colloid Interface Sci.* 490, 754–761.
- Li, Z., Kong, Y., Ge, Y., 2015. Synthesis of porous lignin xanthate resin for Pb²⁺ removal from aqueous solution. *Chem. Eng. J.* 270, 229–234.
- Lin, Y., Reino, C., Carrera, J., Perez, J., Van Loosdrecht, M.C.M., 2017. Glycosylated amyloid-like proteins in the structural extracellular polymers of aerobic granular sludge enriched with ammonium-oxidizing bacteria. *Microbiol. Open* e616, 1–14.
- Liu, W., Zhang, J., Jin, Y., Zhao, X., Cai, Z., 2015. Adsorption of Pb(II), Cd(II) and Zn(II) by extracellular polymeric substances extracted from aerobic granular sludge: efficiency of protein. *J. Environ. Chem. Eng.* 3, 1223–1232.
- Liu, X., Chen, Q., Zhu, L., 2016. Improving biodegradation potential of domestic wastewater by manipulating the size distribution of organic matter. *J. Environ. Sci. (China)* 47, 174–182.
- Long, B., Xuan, X.P., Yang, C.Z., Zhang, L.N., Cheng, Y.Y., Wang, J.Q., 2019. Stability of aerobic granular sludge in a pilot scale sequencing batch reactor enhanced by granular particle size control. *Chemosphere* 225.
- Metcalf & Eddy, I., Tchobanoglous, G., Stensel, H.D., Tsuchihashi, R., Burton, F., 2014. *Wastewater engineering: Treatment and Resource Recovery*. McGraw-Hill Education.
- Morgenroth, E., Sherden, T., Van Loosdrecht, M.C.M., Heijnen, J.J., Wilderer, P.A., 1997. Aerobic granular sludge in a sequencing batch reactor. *Water Res.* 31 (12), 3191–3194.
- Quoc, B.N., Armenta, M., Carter, J.A., Bucher, R., Sukapantharam, P., Bryson, S.J., Stahl, D.A., Stensel, H.D., Winkler, M.-K.H., 2021. An investigation into the optimal granular sludge size for simultaneous nitrogen and phosphate removal. *Water Res.* 198.
- Pronk, M., De Kreuk, M.K., de Bruin, B., Kamminga, P., Kleerebezem, R., Van Loosdrecht, M.C.M., 2015. Full scale performance of the aerobic granular sludge process for sewage treatment. *Water Res.* 84, 207–217.
- Tjihuis, L., Van Loosdrecht, M.C.M., Heijnen, J.J., 1994. Formation and growth of heterotrophic aerobic biofilms on small suspended particles in airlift reactors. *Biotechnol. Bioeng.* 44, 595–608.
- Toja Ortega, S., Pronk, M., De Kreuk, M.K., 2021. Anaerobic hydrolysis of complex substrates in full-scale aerobic granular sludge: enzymatic activity determined in different sludge fractions. *Appl. Microbiol. Biotechnol.* 105 (14–15), 6073–6086.
- Toja Ortega, S., van den Berg, L., Pronk, M., De Kreuk, M.K., 2022. Hydrolysis capacity of different sized granules in a full-scale aerobic granular sludge (AGS) reactor. *Water Res.* X, 16.
- Van den Berg, L., Kirkland, C.M., Seymour, J.D., Codd, S.L., Van Loosdrecht, M.C.M., De Kreuk, M.K., 2020. Heterogeneous diffusion in aerobic granular sludge. *Biotechnol. Bioeng.* 117 (12), 3809–3819.
- Van den Berg, L., Toja Ortega, S., Van Loosdrecht, M.C.M., De Kreuk, M.K., 2022. Diffusion of soluble organic substrates in aerobic granular sludge effect of molecular weight. *Water Res.* 16, 100148.
- Van Dijk, E.J.H., Haaksman, V.A., Van Loosdrecht, M.C.M., Pronk, M., 2022. On the mechanisms for aerobic granulation - model based evaluation. *Water Res.* 216, 118365.
- Van Dijk, E.J.H., Pronk, M., Van Loosdrecht, M.C.M., 2020. A settling model for full-scale aerobic granular sludge. *Water Res.* 186, 116135.
- Wei, S.P., Stensel, H.D., Nguyen Quoc, B., Stahl, D.A., Huang, X., Lee, P.H., Winkler, M. H., 2020. Flocs in disguise? High granule abundance found in continuous-flow activated sludge treatment plants. *Water Res.* 179, 115865.

- Winkler, M., Van Loosdrecht, M.C.M., 2022. Intensifying existing urban wastewater aerobic granular sludge offers improvements to treatment processes. *Science* 375 (6579), 377–378.
- Winkler, M.K., Kleerebezem, R., Khunjar, W.O., de Bruin, B., Van Loosdrecht, M.C.M., 2012. Evaluating the solid retention time of bacteria in flocculent and granular sludge. *Water Res.* 46 (16), 4973–4980.
- Yang, B., Liang, W., Bin, L., Chen, W., Chen, X., Li, P., Wen, S., Huang, S., Tang, B., 2023. Insights into the life-cycle of aerobic granular sludge in a continuous flow membrane bioreactor by tracing its heterogeneous properties at different stages. *Water Res.* 243, 120419.
- Zaghloul, M.S., Achari, G., 2022. A review of mechanistic and data-driven models of aerobic granular sludge. *J. Environ. Chem. Eng.* 10 (3).
- Zhang, B., Qi, B.W., Shi, W.X., Huang, S.C., Xu, W., Yan, P., Zhang, B., Lens, P.N.L., Peng, Y.Z., 2025. Impaired denitrification of aerobic granules in response to micro/nanoplastic stress: insights from interspecies interactions and electron transfer process. *Water Res.* 279, 123472.
- Zhou, R., Li, H., Liu, C., Liu, Y., Lee, J.-F., Lin, Y.-J., Yan, Z., Xu, Z., Yi, X., Feng, C., 2023. Magnetic anaerobic granular sludge for sequestration and immobilization of Pb. *Water Res.* 239, 120022.